

Neural network analysis for sacrificial cathodic protection of steel embedded in concrete

Thirumalai Parthiban^a, R.Ravi, G.T.Parthiban, N.Palaniswamy and V.Sivan^b
Central Electrochemical Research Institute (CECRI), Karaikudi 630 006, India

Abstract

Durability of concrete significantly depends on protecting the embedded steel against corrosion. Among the various methods available for protecting the steel, cathodic protection is widely adopted. Effectiveness of cathodic protection the steel in concrete is determined from the potential of the steel and the current flowing to maintain the protective potential.

The measurement of the potential must be accurate to confirm the protection of the steel. Automation of potential measurement at several points and their averaging will remove manual errors. To achieve this, a data acquisition system for continuously monitoring and measuring the potential of the steel in concrete was designed. Appropriate software was also developed. Using this system, potential of the steel was measured on concrete slabs, with and without cathodic protection. This software included the neural network analysis for analyzing the data from these slabs. Excellent agreement was found between the output data and the predicted data.

Keywords: Steel reinforced concrete, Cathodic protection, Magnesium anode, Potential monitoring, Neural network analysis, Prediction

a: Corresponding author Email: thirumalaip@yahoo.com Phone: +91-4565-227550

b: National Institute of Technology (NIT), Trichy, India

The phenomenon of corrosion and the methods for its control are widely studied [1]. Among the various corrosion control methods available, impressed current cathodic protection is a major technique adopted to control the corrosion of steel embedded in concrete [2-7]. Sacrificial cathodic protection is less widely employed for protecting the steel in concrete [8]. This method involves coupling the metal to be protected with a more active metal which will serve as the anode. It does not require external source for power supply. The most commonly used anodes are alloys based on magnesium, aluminium and zinc [9].

Generally, cathodic protection must be properly monitored and maintained to ensure its effectiveness. Detection of corrosion of steel embedded in concrete as a function of its potential is an electrochemical approach, which is of paramount importance in this study [10-14]. The predictions and the derived parameters of the present study are compared with those of ASTM C876-91 and Offshore Technology Reports [15-16]. Ultimately, the measurement duration is reduced to a minimum without compromising the accuracy, which is the main purpose for this study.

Towards this direction, a multi-channel data acquisition system was built using National Instruments data acquisition card (AT-MIO-16E-10) to acquire the potential of embedded steel from different concrete slabs. The data obtained were analyzed using the software developed based on neural network analysis. The details of the data acquisition system and measurement procedure adopted are elaborated in our earlier paper [17].

Artificial neural networks (ANN) are mathematical systems that simulate biological neural networks. ANN consists of three processing elements viz. input neurons, hidden neurons and output neurons, organized in layers, which process information by their dynamic response to external inputs [18-21]. To predict the

potential of the steel in concrete, a typical feed-forward neural network with back-propagation method was developed [22–26]. The software for back-propagation neural network (BPNN) was developed using supervisory learning method, gradient descent rule (for error minimization) and sigmoid transfer function. More details on the neural network method applied and data analysis procedures are reported in our earlier publications [27-28].

2. Experimental

For the present study, steel reinforced concrete slab of size 1 m x 1 m x 0.4 m was used. 3.5% sodium chloride by weight of cement was added during casting. Steel rod of 10 mm diameter was used as the reinforcement.

Magnesium alloy sacrificial anode [Iron: 0.03% (max.), Copper: 0.005% (max.), Manganese: 0.185 %, Zinc: 4.17 %, Aluminium: 6.33 % and Magnesium: Balance] was designed for sacrificial cathodic protection of the embedded steel in this slab for 36 months. It was embedded at the center of the slab. The steel assembly, embedded in the concrete, was connected to the anode at diagonally opposite ends and cathodic protection was activated [29]. The slab was left in open air and wetted uniformly, every day. Potential of the embedded steel and the current flowing in the slab was periodically measured and analyzed.

Fig.1 illustrates the measurement unit incorporating the data acquisition system connected to the reference electrode assembly for monitoring the cathodically protected slab. Copper/Copper sulphate reference electrode was used as the reference electrode.

Software modules were developed for potential data acquisition and analysis. Among the sixteen channels available in the data acquisition card, the data acquisition system built for the study used six channels. The six selected channels were linked to six different Copper/Copper sulphate electrodes, fixed on the movable

platform designed and the potential was acquired for about 28600 h, at specific time intervals.

36 different nodal points were marked on the surface of the slab for measuring the potential of the embedded steel at different distances from the anode. The potentials obtained at various points corresponding to each distance from the anode, were averaged for the specific distance. The potential data acquired were analyzed using back propagation neural network (BPNN) for each distance from the anode. Data acquired were divided into two different sets, one for the range 0 to 3200 h and the other for the range 0 to 10000 h, for analysis. From these sets, data were selected for the corresponding training set and the test set. The number of neurons in the input layer and the output layer were determined by the number of input and output parameters. Simultaneously, the number of neurons in the hidden layer(s) was varied. The neural net used the training set with the locations and time interval as the input data for predicting the potential as the output data. Thus, the BPNN was trained and optimized for predicting the potential of steel with sacrificial cathodic protection.

The pattern of potential shift obtained in this slab was compared with reported literature, to ascertain the cathodic protection offered to this slab [27]. The results obtained by prediction from the neural network for this slab were also compared with the measured values. By predicting and comparing the potentials obtained at different time intervals randomly, the validity of the recognized / predicted pattern was confirmed.

3. Results and Discussion

The data acquired from slab at the end of each time interval, at five different distances from the anode ranging from 28 to 57 cm, was averaged by the software for each specific distance. It is important to note that the data at different distances

corresponding to different locations were acquired simultaneously. The averaged potential for each distance was plotted against the corresponding time of measurement and is illustrated in fig. 2. It is evident from the figure that the potential of the steel initially varied from -490 to -540 mV at all distances. With increase in time, the potentials shifted towards less negative values with lesser variations. The slabs were monitored using the data acquisition and processing system up to 28600 h.

During the initial stages, when the potential variations were considerably large, a set of training data up to 3200 h was chosen for analysis, for a distance of 28 cm from anode. From this set, data were selected randomly for training and testing [30-34]. The test data selected were in the lower range for estimation and extrapolation up to ~ 8000 h. These timings were chosen in such a manner that they are beyond those assigned for the training data, similar to extrapolation. This was carried out in order to verify the different claims made elsewhere [33, 35]. Data selected was normalized from 0 to 1, before training and testing.

The training data was used to determine the number of neurodes in the hidden layer, which resulted in the least error between the calculated neural network output and the experimentally measured data. Different number of neurodes in the hidden layer was evaluated and their resulting root mean squared (RMS) error was determined. From this, the number of neurodes exhibiting minimum error was selected and plotted. It can be seen from fig. 3 that the error was minimum when the number of neurodes was 14. The next step involved the identification of the number of cycles (training periods) showing the lowest error for this minimum number of neurodes. Hence, the number of cycles was chosen to be 93, which showed the lowest error value, as in fig. 4. Artificial neural network with an input layer having two

neurodes (time and distance), a hidden layer with 14 neurodes and an output layer with one neurode (potential) was thus identified for analyzing the test data. For this network architecture, the highest error was only about 5.63 %, which is an encouraging observation.

Using this network architecture, neural network outputs (predicted potentials) for different time intervals (designated as test data and that were not used in the training) were determined. The potentials predicted by the neural network were plotted along with the experimentally measured potentials for the corresponding times and are shown in fig. 5. It is observed that the deviations of these predicted potentials from the experimentally measured potentials, up to ~8000 h, is low and is only about 5.63 %, as mentioned earlier. In addition, the developed neural network was able to closely follow the experimental data, which confirms the validity of the network for estimation and prediction. Similarly the neural network outputs (predicted potentials) for both the training and test data were observed to fit well with the experimental data.

The neural network processing, as described above for the distance of 28 cm from anode, was carried out for the other four remaining distances from the anode as well. The experimentally measured potentials and the predicted potentials for corresponding times are shown in fig. 6 to fig. 9, for these distances from the anode. The deviation of the predicted potentials from the experimentally measured values is very low.

This is illustrated in fig. 10 where the deviation of predicted potential values for different times of measurement from the experimentally measured values for the corresponding times of measurement, at different distances from the anode (acquired data) is plotted. The correlation between the predicted data and the

experimental data was observed to be very high for all the distances from the anode.

The coefficient of correlation varied from 0.81 to 0.92. These observations are in good agreement with similar investigations using neural networks [35-36].

The accuracy of prediction with data over a longer time range was evaluated using another set of data, to enhance the prediction accuracy. Here the training data was selected over the range up to 10000 h for all distances from the anode, to facilitate the extension of the predicted range up to 26000 h. A longer range implies more number of data and hence more will be the accuracy of prediction by the neural network. The procedures to evaluate the number of neurodes in the hidden layer and training cycles adopted were identical to those for the 3200 h range of data, based on minimum error. The number of neurodes in the hidden layer was determined to be 2, as illustrated in fig. 11 and the number of cycles was determined to be 2000, as shown in fig. 12, for this set of data.

With this network architecture, neural network outputs (predicted potentials) for the test data were evaluated. The results obtained are illustrated in fig. 13 to 17, for all the distances from the anode. Here, it is observed that the predicted potential values are much more close to the experimentally measured potentials.

The predicted potential values for different times of measurement were plotted against those of the experimentally measured potentials for the corresponding times of measurement, which is shown in fig. 18. The correlation coefficients for all the distances from the anode were evaluated. These ranged from 0.861 to 0.977, confirming excellent fit. From these figures, it can be seen that the training data chosen for longer range yields a much better fit with the experimentally measured

data. These techniques can be extended beyond the laboratory studies, for on-line process analysis and field studies, which is the significance and flexibility of ANN.

4. Conclusions

On comparing the potential of steel in the cathodically protected slab with those reported, the corrosion of the steel is observed to be arrested.

The corrosion in this slab is insignificant even during the initial stages as the embedded steel is rendered to be the cathode.

The neural network approach employed in this study was able to predict the potential of the steel embedded in concrete with respect to time, with considerable accuracy.

Further, the predicted potential values exhibit excellent fit with the experimentally measured values, as indicated by the very high correlation coefficients (0.81 to 0.97).

It also identified whether the predicted potential lies in the corroding regime or not and in turn confirmed the effectiveness of cathodic protection.

5. References

- [1] H.H. Uhlig and R.W. Revie, "Corrosion and Corrosion Control: an Introduction to Corrosion Science and Engineering", by Fourth Ed., John Wiley & Sons Inc., New Jersey, 2008.
- [2] L. Bertolini, F. Bolzoni, A.Cigada T.Pastore and P.Pedefferri, Corrosion Science, 35 (1993) 1633.
- [3] M. McKenzie, Research Report 328, Transport and Road research Laboratory, Dept of Transport, Crowthorne, Berkshire, UK ,1991.
- [4] K.M. Howell, Materials Performance, 32 (1993) 16.
- [5] N.C. Webb, Construction of Building Materials, 6 (1992) 179.
- [6] P.J. Jurach, Report No. FHWA-DP34-2, California Department of Transportation, 1982.
- [7] H.C. Schell, D.G. Manning and K.C. Clear, 63rd Annual Transportation Research Board Meeting, Washington, D.C., 1984.
- [8] W.H. Hartt, Corrosion, 58, 6 (2002) 513.
- [9] John Morgan, 'Cathodic Protection', 2nd Edition, Pub. by NACE International, 1440 South Creek Drive, Houston, Texas 77084, USA, (1987).
- [10] R. Stratfull, Materials Protection, 3 (1968) 29.
- [11] J. P. Broomfield and J. S Tinnea., Report No. SHRP-C/UWP-92-618, 1993.
- [12] J. Bennett and T. Turk, Report No. SHRP-S-359, Strategic Highway Research Program, Washington D.C. 1994.
- [13] L. Bertolini, P. Pedefferri, T. Pastore, B. Bazzoni, and L. Lazzari, Corrosion, 52 (1996) 552.

- [14] RP 0100-2004 Cathodic Protection of Prestressed Concrete, NACE, Houston, Texas, 2004.
- [15] ASTM C876-91, Standard test method for half-cell potentials of uncoated reinforcing steel in concrete, 1999.
- [16] Department of Energy, Offshore technology report: development of inspection techniques for reinforced concrete, Concrete in the oceans series, HMSO, London; 1986.
- [17] Thirumalai Parthiban, R. Ravi and G.T. Parthiban, Advances in Engineering Software, 37 (2006) 375.
- [18] D.E. Rumelhart, G.E.Hinton and R.J. Williams, Parallel Distributed Processing, Explorations in the Microstructure of Cognition, Vol. 1: Foundations, MIT Press, Cambridge, Massachusetts, 1986.
- [19] R. P. Lippman, IEEE ASSP Magazine, 4 (1987) 4.
- [20] P.D. Wasserman, Neural Computing: Theory and Practice, Van Nostrand Reinhold Co., New York, 1989.
- [21] R. Beale and T. Jackson, Neural Computing: An Introduction, Adam Hilger, Bristol, 1990.
- [22] R. Hecht-Nielsen, Neurocomputing, Addison Wesley, 1989.
- [23] P.J. Werbos, The roots of Back-propagation: From ordered derivatives to neural networks and political forecasting, John Wiley & Sons, Chichester, 1993.
- [24] M.T. Hagan, H.B. Demuth and M. Beal, Neural Network Design, PWS, Boston, 1996.
- [25] N.K. Bose, P. Liang, Neural Network Fundamentals, McGraw-Hill, New York, 1996.

- [26] D.W. Patterson, Artificial Neural Networks: Theory and Applications, Simon and Schuster, New York, 1996.
- [27] Thirumalai Parthiban, R.Ravi, G.T.Parthiban, S.Srinivasan, K.R.Ramakrishnan and M.Raghavan, Corrosion Science, 47 (2005) 1625.
- [28] Thirumalai Parthiban, R.Ravi and N.Kalaiselvi, Electrochimica Acta, 53, 4 (2007) 1877.
- [29] G.T. Parthiban, V. Saraswathy, N.S. Rengaswamy, Bull. Electrochem., 16 (2000) 253.
- [30] Marianne Defernez and Katherine Kemsley E., Analyst, 124 (1999) 1675.
- [31] Qianfeng Li, Xiaojun Yao, Xingguo Chen, Mancang Liu, Ruisheng Zhang, Xiaoyun Zhang and Zhide Hu, Analyst, 125 (2000) 2049.
- [32] Sun Gang, Zhou Yongyao, Wang Huaiwen, Chen Hongli, Chen Xingguo and Hu Zhide, Analyst, 125 (2000) 921.
- [33] M.Y Rafiq., G. Bugmann and D.J. Easterbrook, Computers & Structures, 79 (2001) 1541.
- [34] A. Kaveh and H. Servati, Computers & Structures, 79 (2001) 1561.
- [35] J.Cai, S.B.Lyon and R A.Cottis, Corrosion Science, 41(1999) 2001.
- [36] R.A. Cottis and M. Turega, Final report on neural networks for corrosion engineering, EPSRC grant number J48481, UMIST, Manchester, UK, 1997.

Figure Captions:

- Fig. 1: Measurement set up for data acquisition in a sacrificial anode cathodic protection system
- Fig. 2: Measured potential of embedded steel with time, at different distances from Anode – slab3
- Fig. 3: Error generated by different number of neurodes for training data up to 3200 h
- Fig. 4: Error generated by different number of cycles for training data up to 3200 h
- Fig. 5: Validation of Test data with training and experimental data for 28cm
- Fig. 6: Validation of Test data with training and experimental data for 37cm
- Fig. 7: Validation of Test data with training and experimental data for 42cm
- Fig. 8: Validation of Test data with training and experimental data for 49cm
- Fig. 9: Validation of Test data with training and experimental data for 57cm
- Fig. 10: Correlation between the predicted potentials and measured potentials at different distances from anode
- Fig. 11: Error generated by different number of neurodes for training data up to 10000 h
- Fig. 12: Error generated by different number of cycles for training data up to 10000 h
- Fig. 13: Validation of Test data with training and experimental data for 28cm
- Fig. 14: Validation of Test data with training and experimental data for 37cm
- Fig. 15: Validation of Test data with training and experimental data for 42cm
- Fig. 16: Validation of Test data with training and experimental data for 49cm
- Fig. 17: Validation of Test data with training and experimental data for 57cm
- Fig. 18: Correlation between the predicted potentials and measured potentials at different distances from anode



Fig. 1

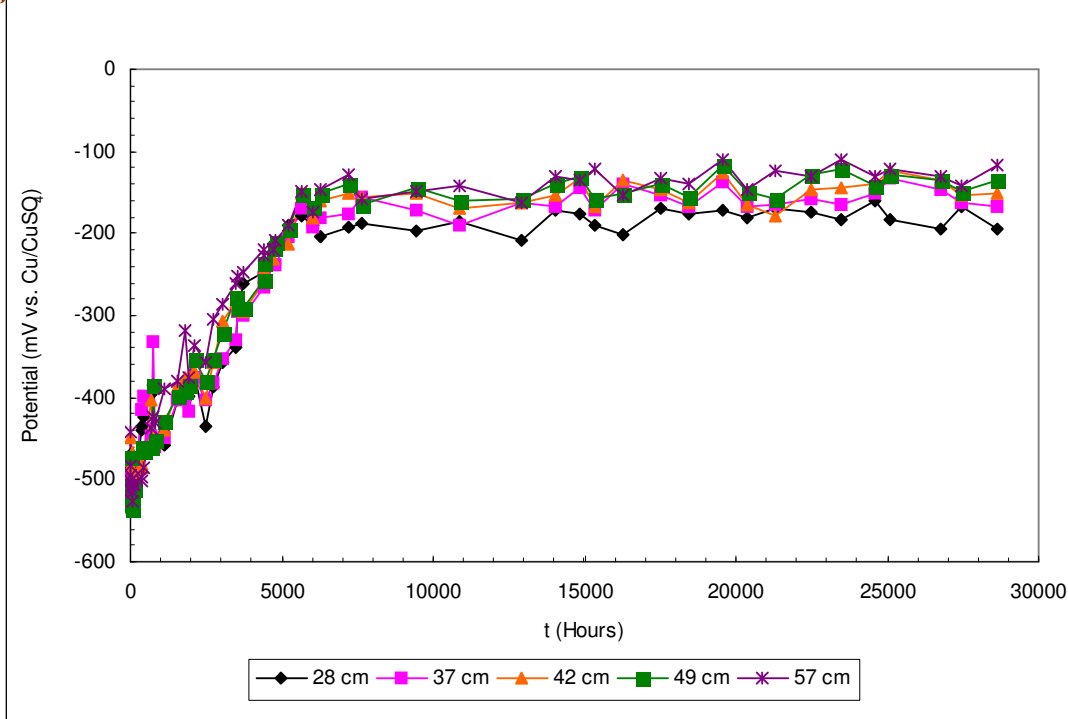


Fig. 2

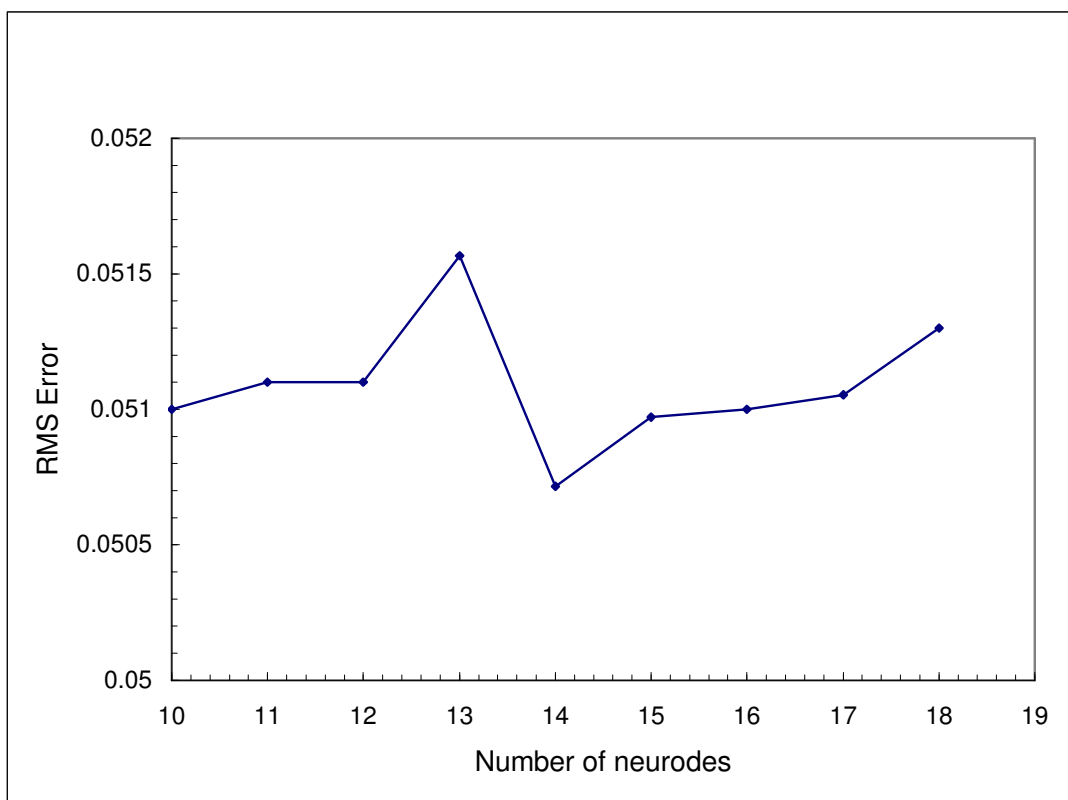


Fig. 3

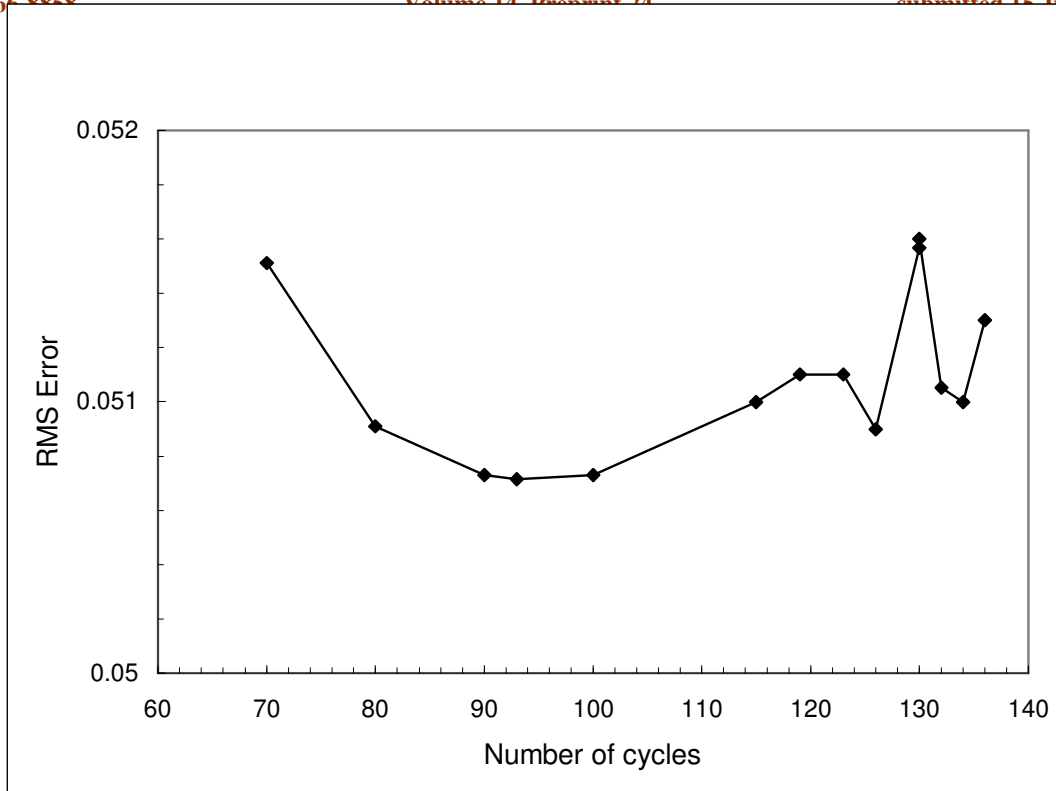


Fig. 4

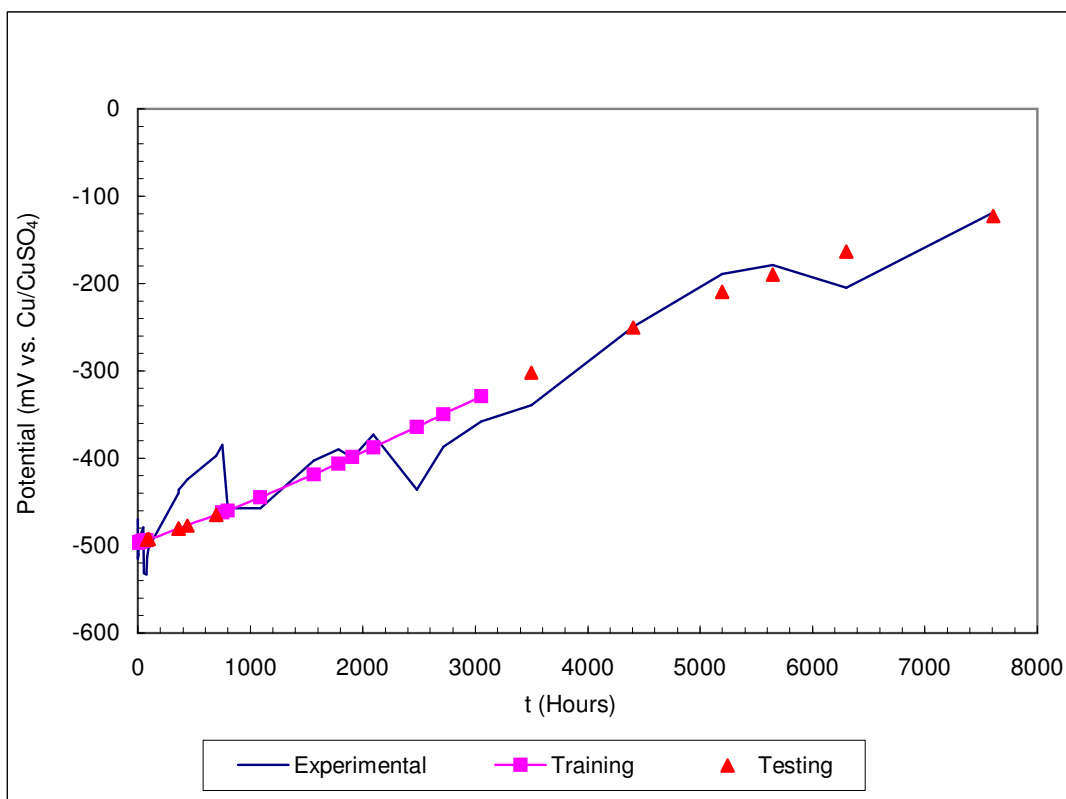


Fig. 5

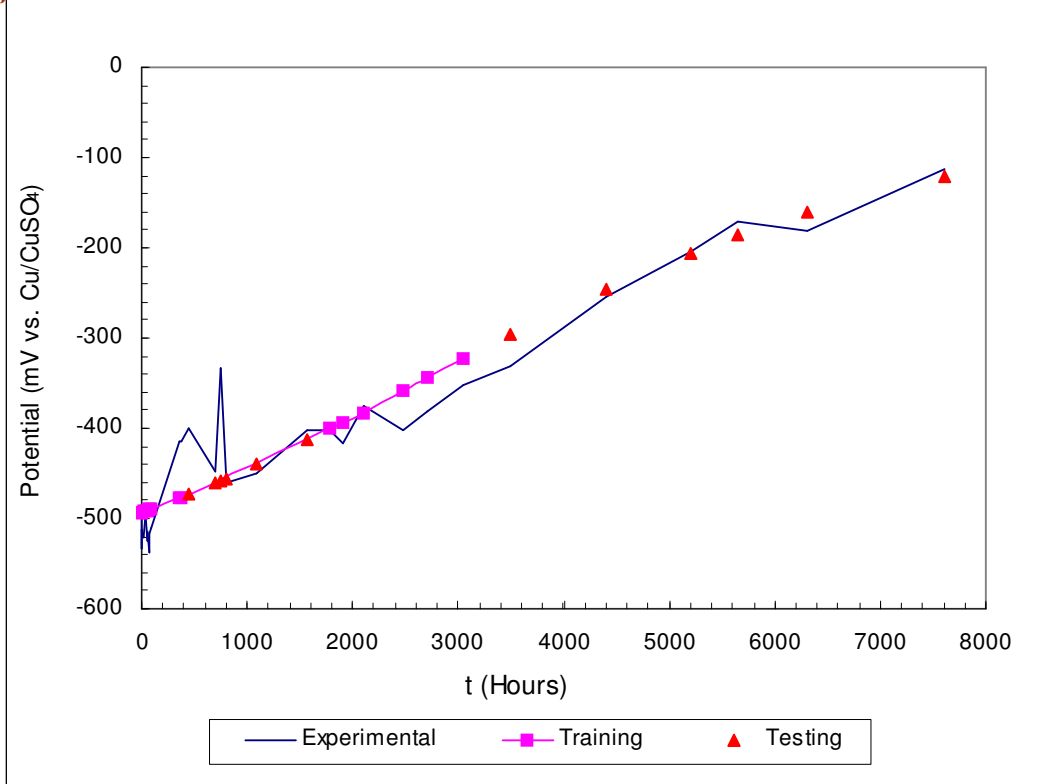


Fig. 6

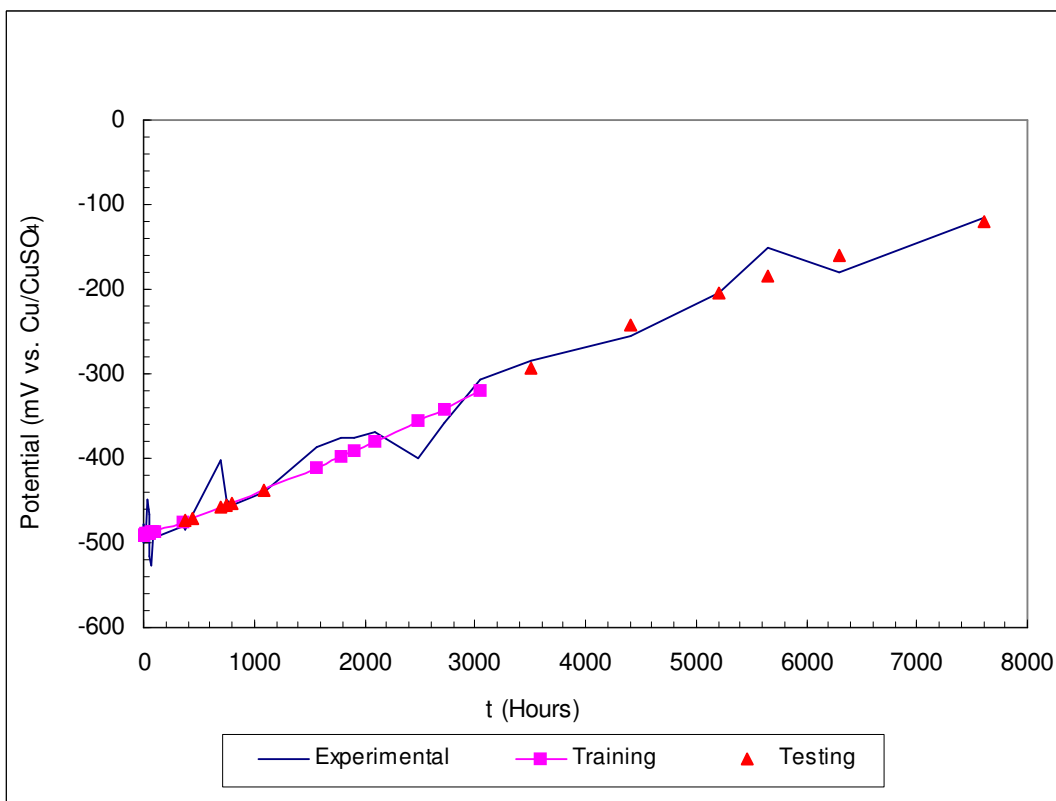


Fig. 7

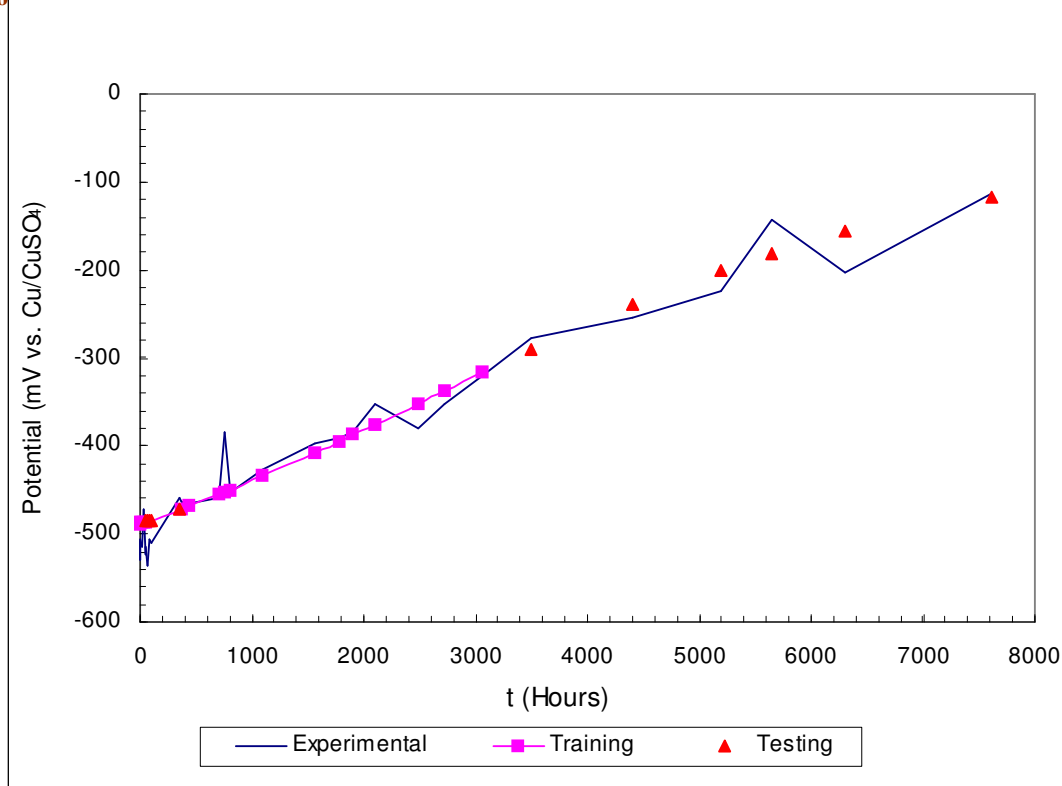


Fig. 8

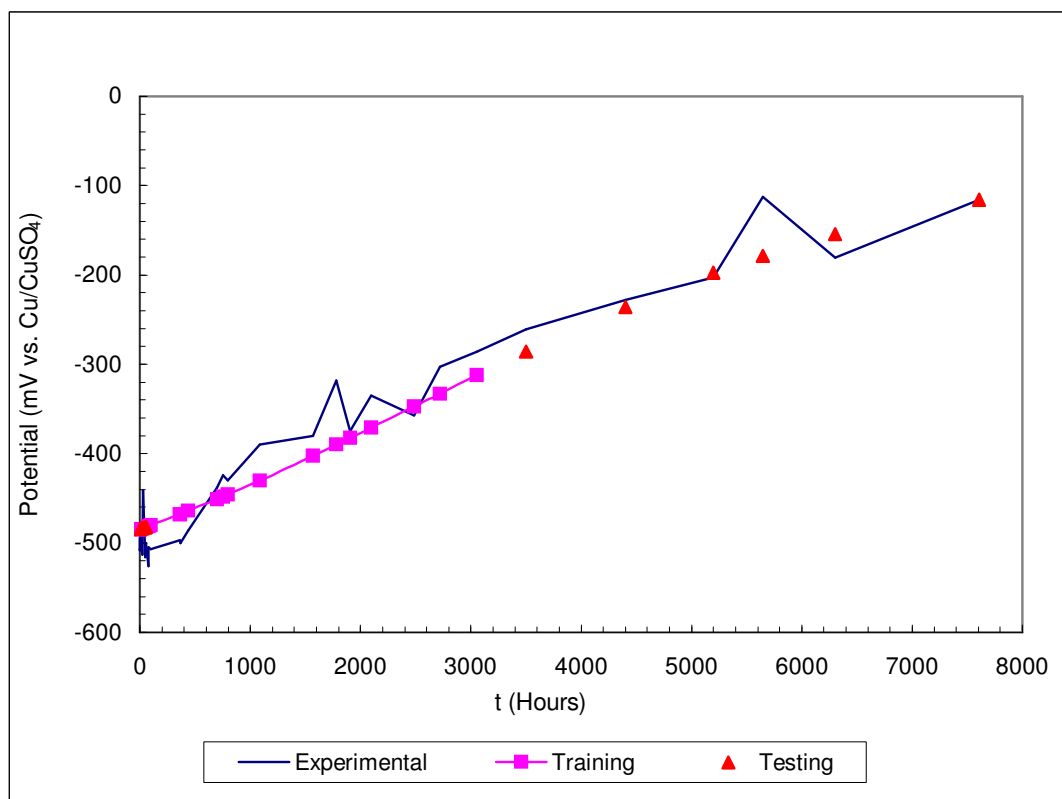


Fig. 9

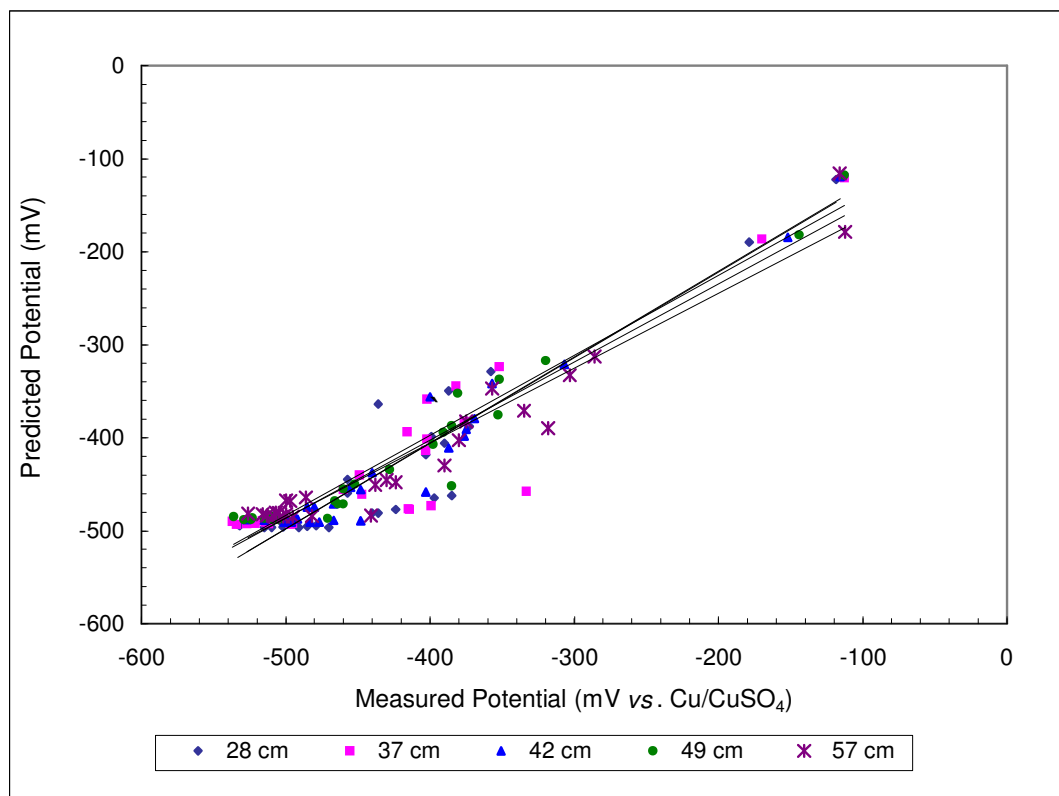


Fig. 10

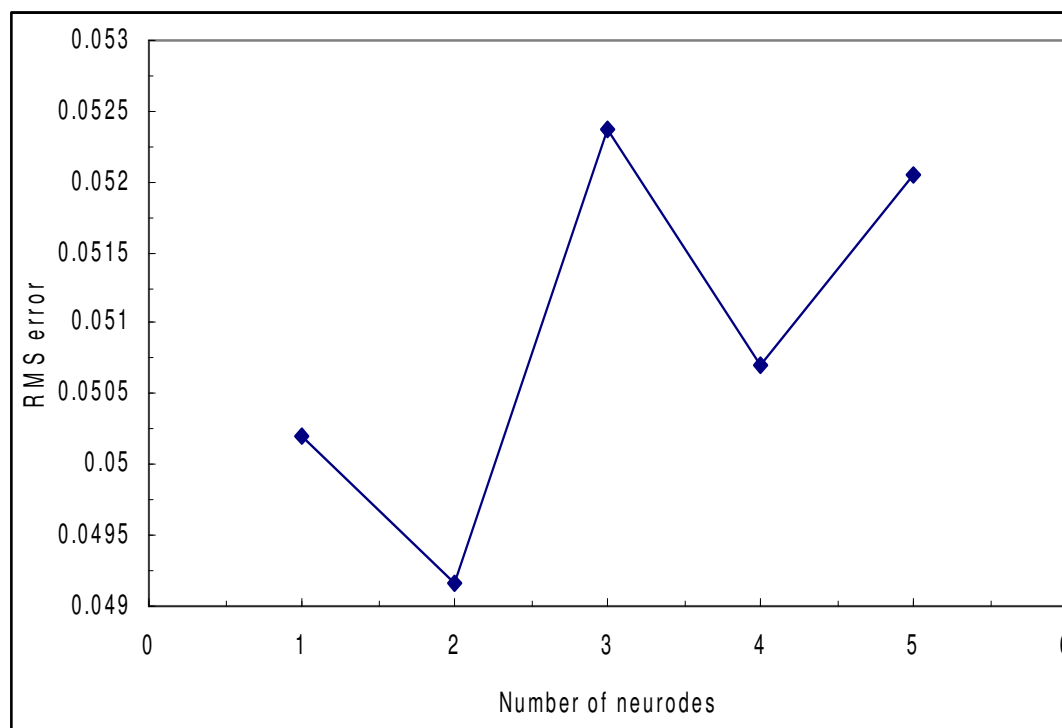


Fig. 11

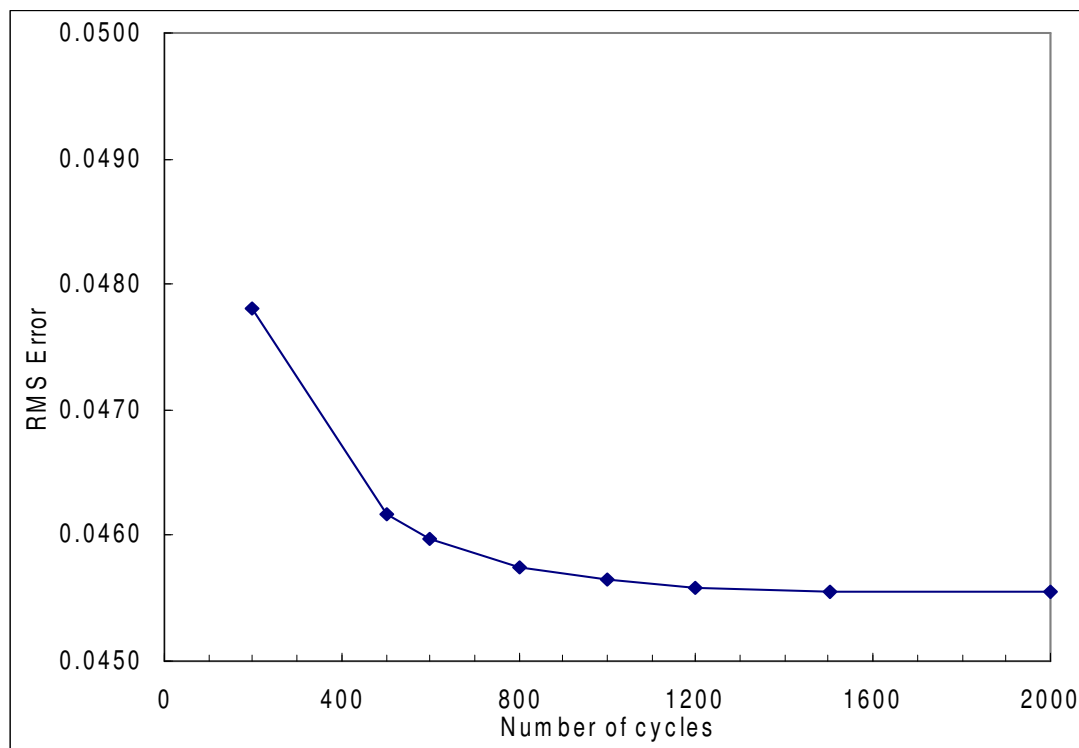


Fig. 12

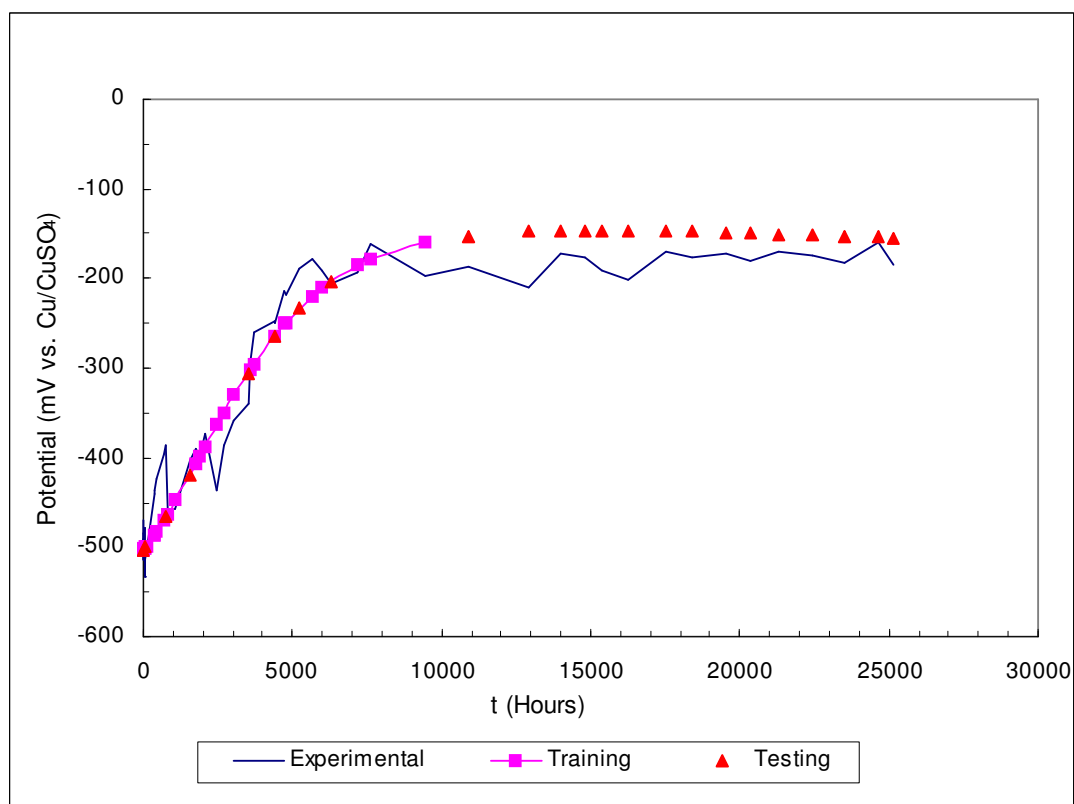


Fig. 13

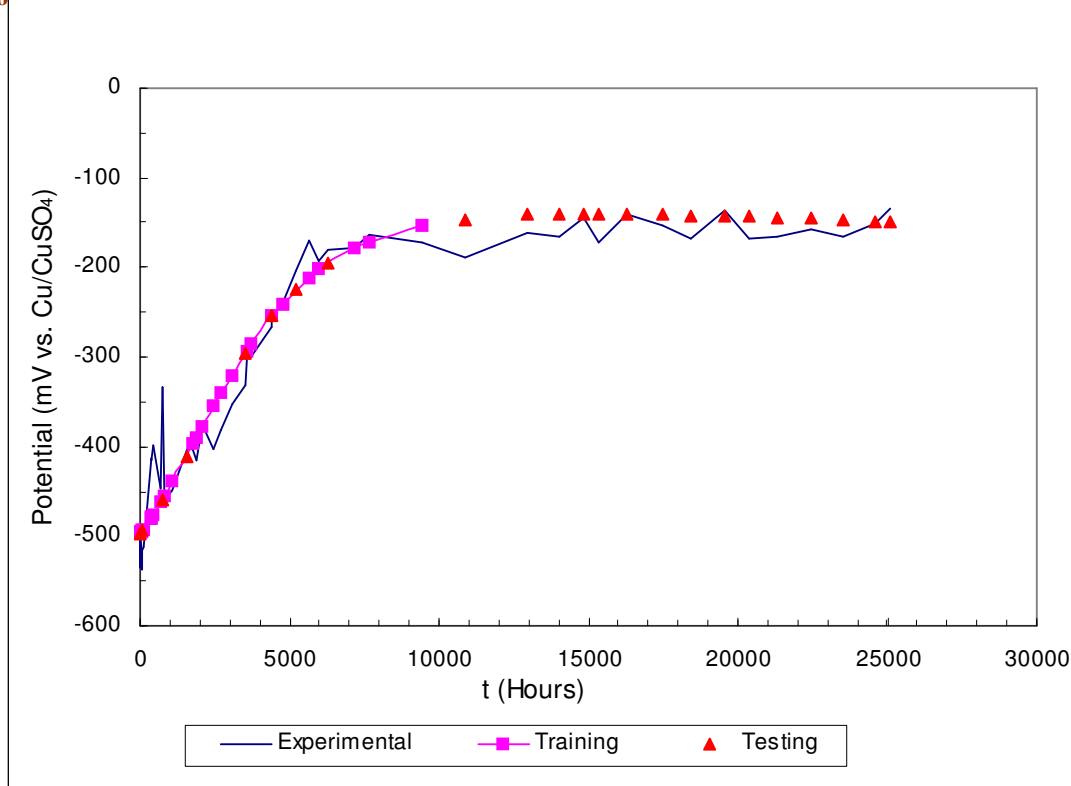


Fig. 14

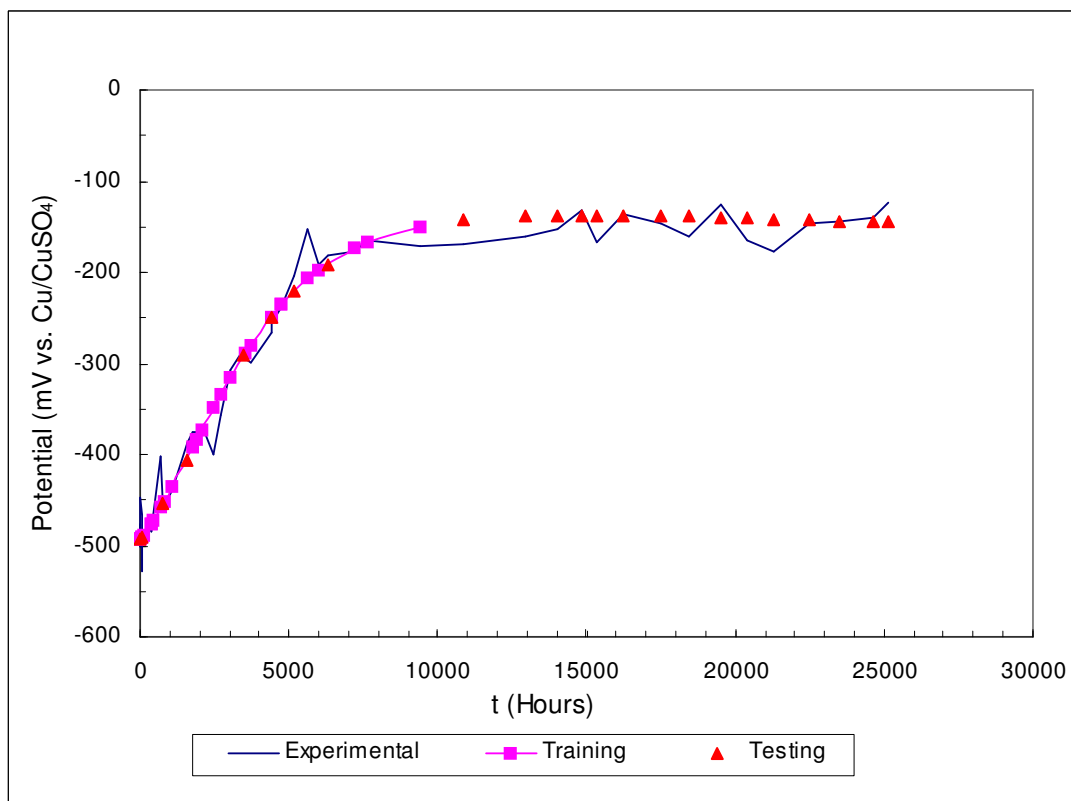


Fig. 15

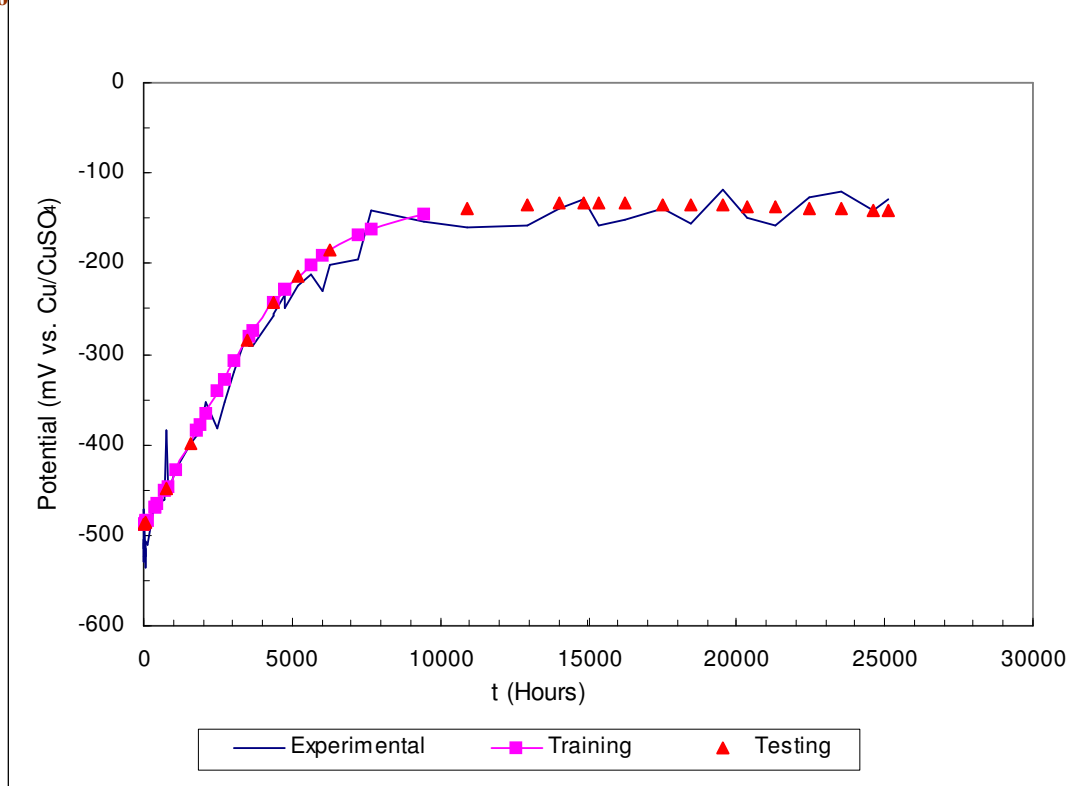


Fig. 16

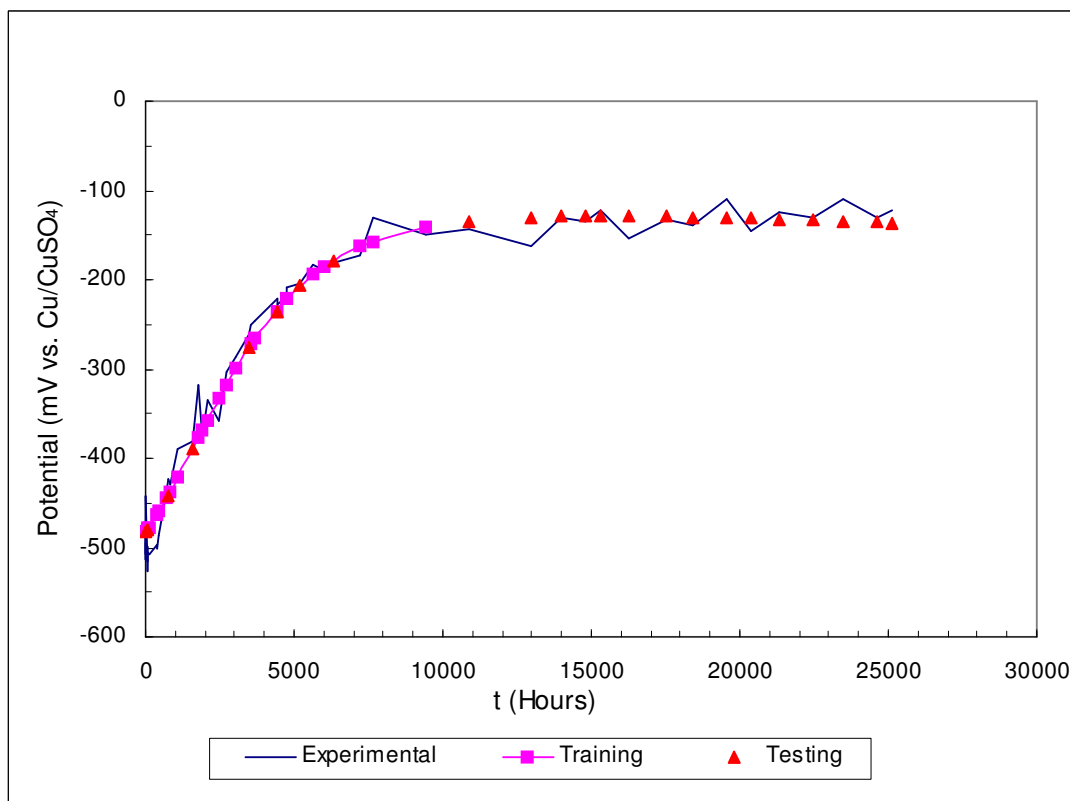


Fig. 17

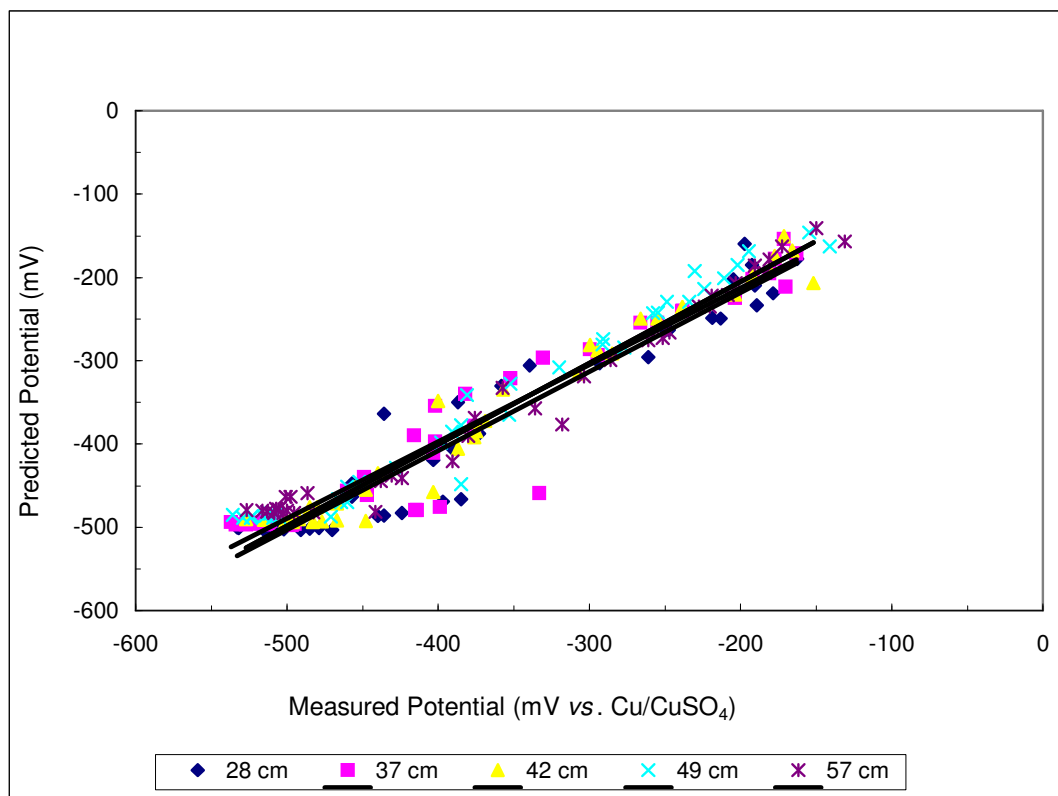


Fig. 18